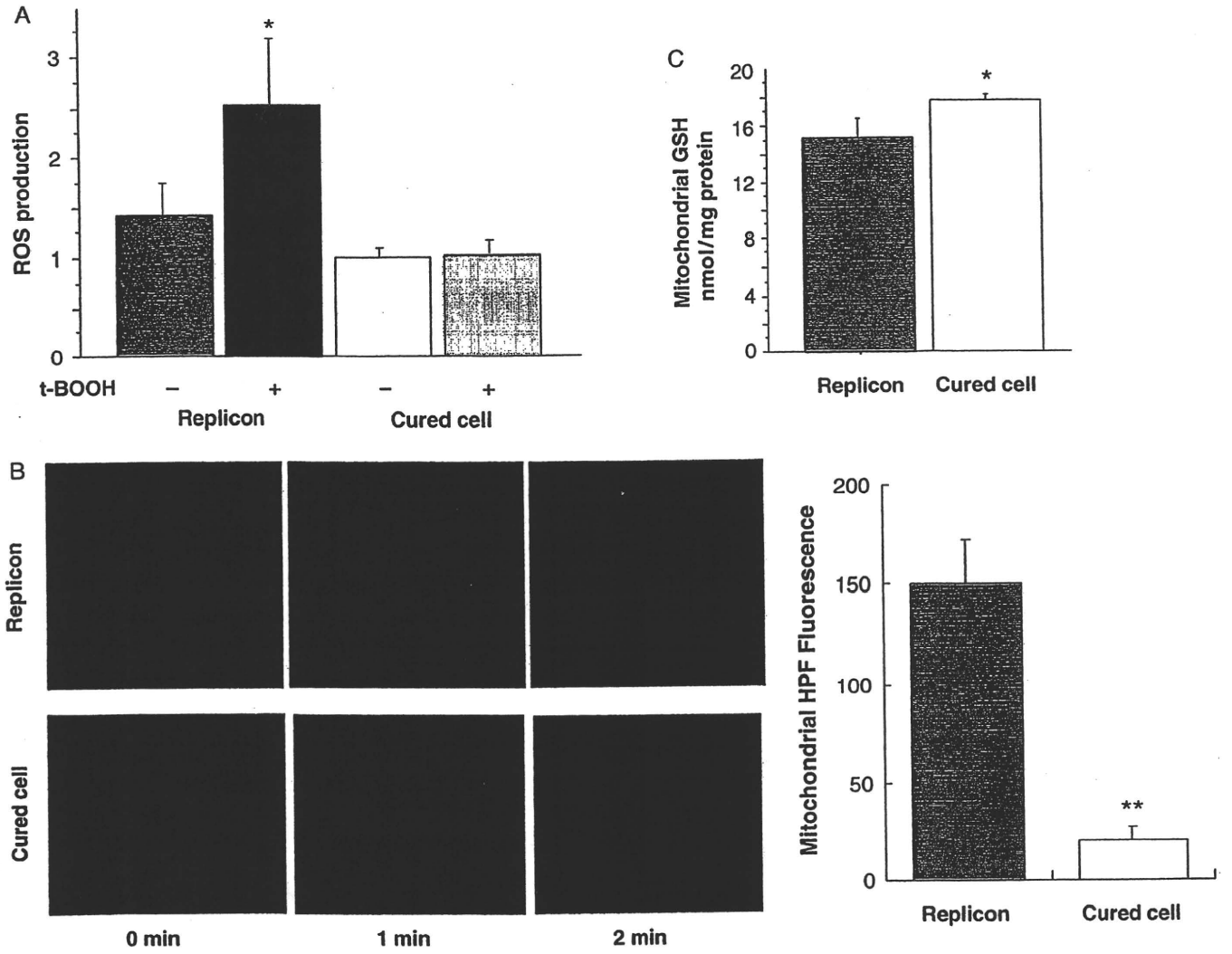

Fig. 1. Effects of HCV replication on ROS production and mitochondrial reduced glutathione level. (A) ROS production was measured by oxidation of DCFDA in HCV replicon cells and cured cells under control conditions or after 5-h incubation with t-BOOH (500 nmol/L). *$P < 0.01$ compared with untreated cured cells. (B) Confocal images of ROS generation. HCV replicon cells and cured cells were pre-incubated with HPF, subsequently treated with t-BOOH (10 nmol/L) and imaged at 30-s intervals. The increase in HPF fluorescence intensity 2 min after treatment with t-BOOH was compared between HCV replicon cells and cured cells. **$P < 0.0005$ compared with HCV replicon cells. (C) Reduced glutathione content was measured in crude mitochondrial fractions prepared from HCV replicon cells and cured cells. *$P < 0.05$ compared with HCV replicon cells. DCFDA, dihydrodichlorocarboxyfluorescein diacetate; HCV, hepatitis C virus; HPF, hydroxyphenyl florescein; ROS, reactive oxygen species.

replicon cells, even though the significance of reduced complex IV activity remains elusive.

Incompletely inhibited hepatitis C virus replication partially restores mitochondrial electron transport activity

Fluvastatin, a 3-hydroxy-3-methylglutaryl co-enzyme A reductase inhibitor, has been shown to have an inhibitory effect on HCV replication in the present full genomic HCV replicon cells (12). We used fluvastatin for partially inhibiting HCV replication in full genomic HCV replicon cells, because it has a lesser inhibitory effect on HCV replication than IFN-α (12). In fact, expression of core protein was present in mitochondria, but was significantly lowered by treatment with fluvastatin in full genomic HCV replicon cells ($P < 0.05$; Fig. 4A). Partial inhibition of HCV replication restored complex I activity by ~13% ($P < 0.05$; Fig. 4B). Although statins including fluvastatin are known to have an anti-oxidative effect (16, 17), treatment with fluvastatin did not improve complex I activity in cured cells (Fig. 4B), suggesting that this activity was restored by its inhibitory effect on HCV replication rather than its anti-oxidative property. However, partial inhibition of HCV replication did

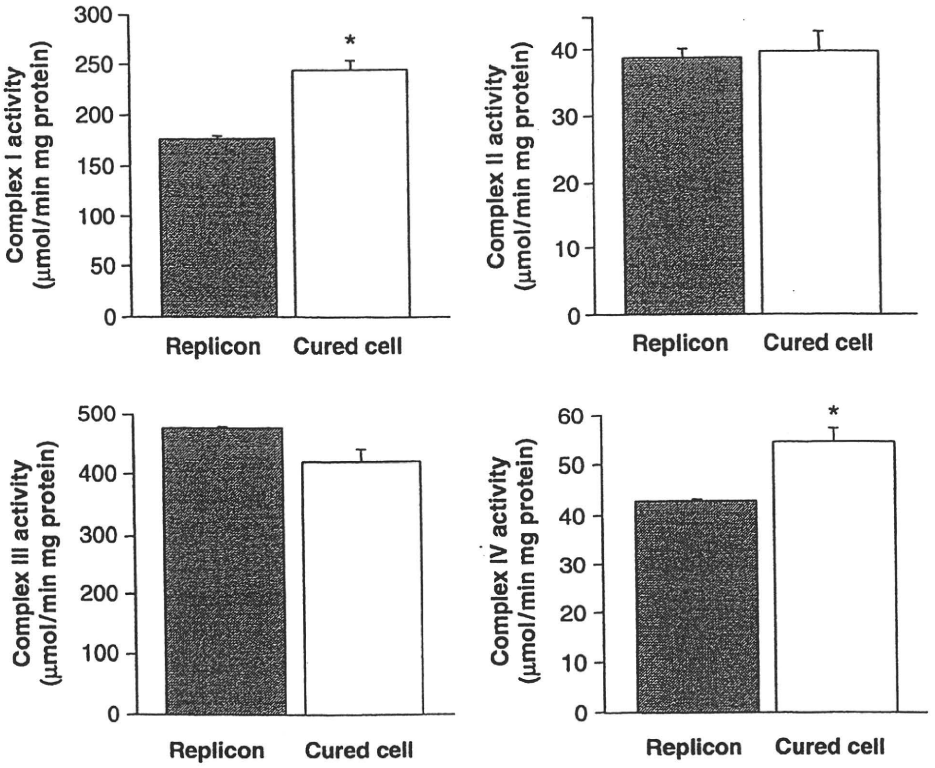

Fig. 2. Mitochondrial complex I, II, III and IV activities. Complex I (NADH-decylubiquinone oxidoreductase) activity, complex II (succinate decylubiquinone 2,6-dichlorophenolindophenol reductase) activity, complex III (ubiquinol cytochrome *c* reductase) activity and complex IV (cytochrome *c* oxidase) activity were measured in submitochondrial fractions prepared from HCV replicon cells and cured cells. $^*P < 0.01$ compared with HCV replicon cells. HCV, Hepatitis C virus; NADH, nicotinamide adenine dinucleotide.

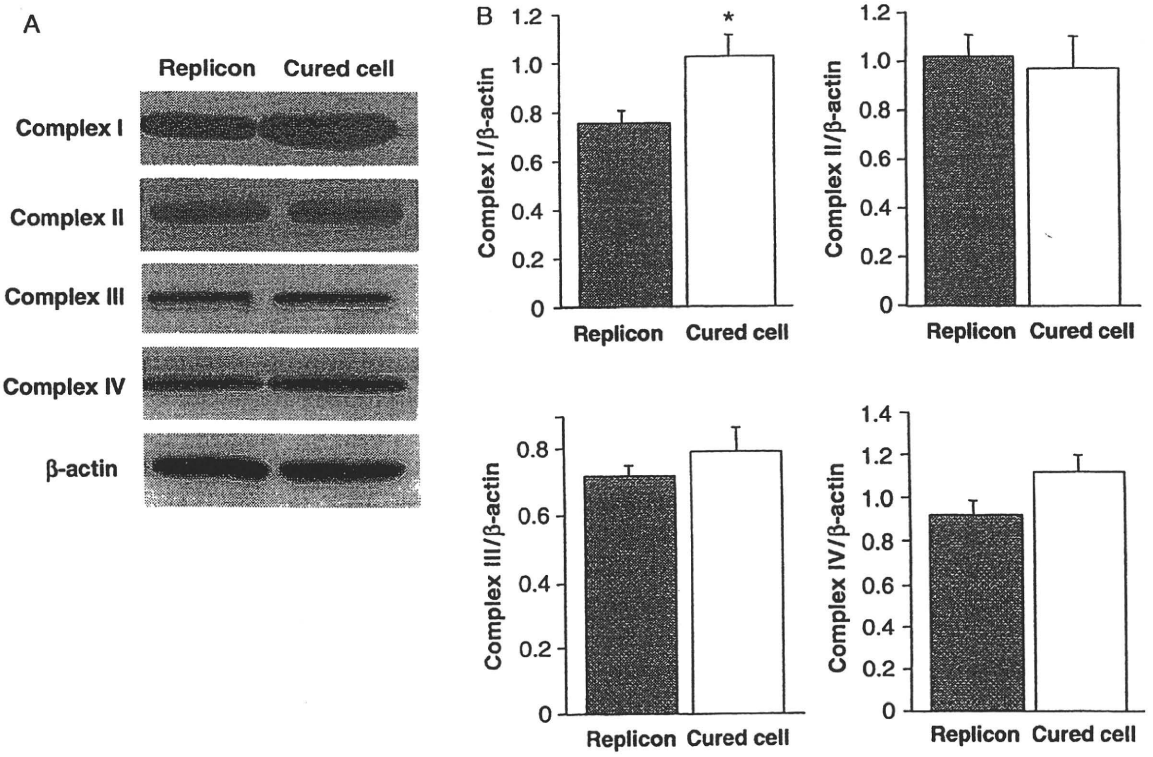

Fig. 3. Expression of mitochondrial complex I, II, III and IV. (A) Immunoblots for complex I, II, III and IV were performed using crude mitochondrial fractions prepared from HCV replicon cells and cured cells. (B) The degree of protein expression was normalized with β-actin protein. $^*P < 0.05$ compared with HCV replicon cells. HCV, hepatitis C virus.

not lead to a significant reduction of ROS production (Fig. 4C), a significantly increased level of mitochondrial reduced glutathione (Fig. 4D) or complex I expression (Fig. 4A). Thus, incomplete inhibition of HCV replication restored mitochondrial electron transport activity in full genomic HCV replicon cells, even though it was not sufficient to reduce mitochondrial oxidative status.

Discussion

We have previously reported that HCV core protein inhibits mitochondrial electron transport and increases ROS production in the transgenic mouse liver (9). Our present results have shown that these phenomena can be reproduced in the presence of HCV replication. As replication of a full-length HCV genome rather than mere core protein expression is closer to the disease condition occurring in patients with chronic hepatitis C, the present results have strengthened the possibility that mitochondrial oxidation, ROS production and inhibition of mitochondrial electron transport are actually caused in chronic hepatitis C. Thanks to the establishment of HCV replicon cells, we could investigate the effect of inhibiting HCV replication on mitochondrial electron transport activity that was closely related to ROS production. In the present study, we focused on restoration of mitochondrial electron transport activity by inhibiting HCV replication, regarding complete inhibition of HCV replication *in vitro* as that of HCV eradicated with IFN therapy and partial inhibition of HCV replication *in vitro* as that in cells undergoing IFN therapy without HCV eradication.

Consistent with a previous observation, complex I activity, but not complex III activity, was reduced in full genomic HCV replicon cells. Complex I appeared to be the source of HCV-induced ROS, because mitochondrial ROS generation can occur at either complex I or complex III (18–20). We also found decreased expression of complex I in full genomic HCV replicon cells as compared with cured cells. Complex I is the site most sensitive to oxidative damage of the electron transport carriers, and inhibition of complex I occurs during the early stages of mitochondrial damage (21). Increased mitochondrial ROS production due to reduction of complex I activity amplifies mitochondrial oxidation, which in turn may inhibit the expression of complex I. Complex IV activity, i.e. that of cytochrome *c* oxidase, was reduced in full genomic HCV replicon cells as well. Complex IV localizes at the end of mitochondrial electron transport, accepts one electron at a time from cytochrome *c* and passes them four at a time to oxygen. Therefore, decreased activity of complex IV may amplify mitochondrial ROS production, possibly by inhibiting electron flow in the respiratory chain.

Thus, it is likely that HCV replication increases mitochondrial ROS production through inhibition of electron transport, causing oxidative stress within the liver in patients with chronic hepatitis C. Several different experimental models of HCV protein expression reproduced this finding (6–8). However, whether reduction of HCV replication restores mitochondrial function remains unknown. In the present study full genomic HCV replicon cells had ~30% reduction of complex I activity ($P = 0.0001$) and ~20% reduction in complex IV activity ($P < 0.01$) as compared with cured cells (Fig. 2). In other words, complete inhibition of HCV replication by IFN-α restored the activities of complex I and complex IV, leading to reduced ROS production in the presence of an exogenous oxidant and to an increase of mitochondrial reduced glutathione content (Fig. 1). There have been several lines of clinical evidence suggesting that HCV elimination by IFN treatment reverses the progression of liver fibrosis and significantly suppresses the development of HCC afterwards (22, 23). Restoration of mitochondrial electron transport activity by complete inhibition of HCV replication may well account for this clinical evidence, because the progression of liver fibrosis and development of HCC in chronic hepatitis C have been shown to be closely related to excess oxidative stress within the liver (24, 25).

In the clinical setting, however, HCV eradication by combination therapy with peginterferon-α and ribavirin has been successful in 50–60% of patients with refractory chronic hepatitis C at most (2, 3). Therefore, it is a critical issue for patients for whom this is unsuccessful if needed, whether prolonged reduction of HCV replication, not elimination of HCV, reduces or delays the progression of liver fibrosis and development of HCC. Although there have been several studies suggesting the inhibitory effect of IFN therapy on HCC development in patients with HCV-associated chronic liver diseases (26, 27), it is still controversial (28). Cured cells did not show core protein expression at all (data not shown), whereas fluvastatin-treated replicon cells had core protein expression that was significantly lower than in replicon cells without treatment. Thus, incomplete inhibition of HCV replication by fluvastatin was useful as a model for assessing if reduction of HCV replication, not elimination of HCV, could restore mitochondrial function. We found that incomplete inhibition of HCV replication restored complex I activity, but did

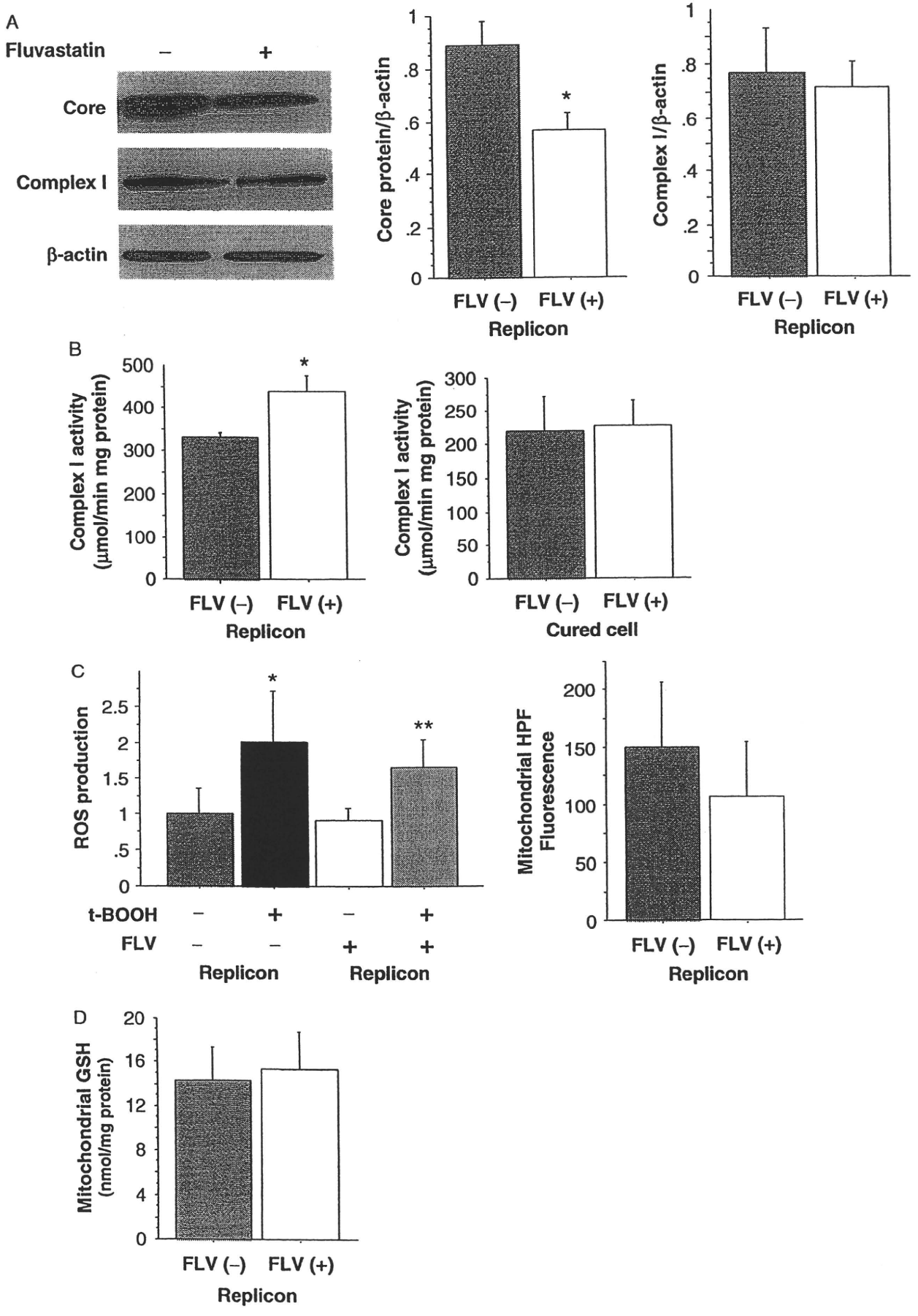

Liver International (2008)

Fig. 4. Effect of fluvastatin on core protein expression, mitochondrial complex I activity and expression, ROS production and mitochondrial reduced glutathione level. (A) Immunoblots for core protein and complex I were performed using crude mitochondrial fractions prepared from HCV replicon cells treated with/without fluvastatin. The degree of protein expression was normalized with β-actin protein. (B) Complex I (NADH-decylubiquinone oxidoreductase) activity was measured in submitochondrial fractions prepared from HCV replicon cells and cured cells, both of which were treated with/without fluvastatin. (C) ROS production was measured by oxidation of DCFDA in HCV replicon cells treated with/without fluvastatin under control conditions or after 5-h incubation with t-BOOH (500 nmol/L). HCV replicon cells treated with/without fluvastatin also were pre-incubated with HPF and subsequently treated with t-BOOH (10 nmol/L). The increase in HPF fluorescence intensity 2 min after treatment with t-BOOH was compared between HCV replicon cells with fluvastatin and those without. $^{*}P < 0.05$ as compared with HCV replicon cells without both t-BOOH and fluvastatin treatment. $^{**}P < 0.005$ as compared with fluvastatin-treated HCV replicon cells without t-BOOH. (D) Reduced glutathione content was measured in crude mitochondrial fractions prepared from HCV replicon cells treated with/without fluvastatin. DCFDA, dihydrodichlorocarboxyfluorescein diacetate; FLV, fluvastatin; HCV, hepatitis C virus; HPF, hydroxyphenyl florescein; NADH, nicotinamide adenine dinucleotide; ROS, reactive oxygen species; t-BOOH, tertiary butyl hydroperoxide.

not lead to the reduction of mitochondrial oxidative status. Thus it should be noted that restoration of complex I activity resulted from the inhibitory effect of HCV replication by fluvastatin rather than its antioxidant property. Even if incomplete inhibition of HCV replication fails to reduce mitochondrial oxidative status *in vitro*, restoration of complex I activity for a certain period *in vivo* may lead to a reduction of mitochondrial oxidative status. However, we need to recognize that inhibition of HCV replication *in vitro* by statins does not necessarily imply the same effect *in vivo*, because the absence of a clinical anti-HCV effect of statins has been reported (29). The present results showing that even incomplete inhibition of HCV replication can restore mitochondrial function to a lesser degree than completely inhibited HCV replication provides us with a rationale for suppressing HCV replication by anti-HCV agents in nonsustained responders to the current combination therapy.

In conclusion, our study shows that HCV replication causes oxidation of the mitochondrial glutathione pool, increases ROS production and inhibits mitochondrial electron transport activity, and that these changes in the mitochondrial redox state can be reversed by reducing HCV replication.

Acknowledgements

This study was supported by grants from the Ministry of Education, Culture, Sports, Science and Technology (No. 15590653 and No. 18590736), and in part by the Ministry of Health, Labor and Welfare, Japan.

References

1. Seeff LB. Natural history of chronic hepatitis C. *Hepatology* 2002; **36**: S35–46.
2. Fried MW, Shiffman ML, Reddy KR, *et al.* Peginterferon alfa-2a plus ribavirin for chronic hepatitis C virus infection. *N Engl J Med* 2002; **347**: 975–82.
3. Davis GL. Current therapy for chronic hepatitis C. *Gastroenterology* 2000; **118**: S104–14.
4. Barbaro G, Di Lorenzo G, Asti AM, *et al.* Hepatocellular mitochondrial alterations in patients with chronic hepatitis C: ultrastructural and biochemical findings. *Am J Gastroenterol* 1999; **942**: 198–205.
5. Valgimigli M, Valgimigli L, Trere D, *et al.* Oxidative stress EPR measurement in human liver by radical-probe technique. Correlation with etiology, histology and cell proliferation. *Free Radic Res* 2002; **36**: 939–48.
6. Okuda M, Li K, Beard MR, *et al.* Mitochondrial injury, oxidative stress, and antioxidant gene expression are induced by hepatitis C virus core protein. *Gastroenterology* 2002; **122**: 366–75.
7. Otani K, Korenaga M, Beard MR, *et al.* Hepatitis C virus core protein, cytochrome P450 2E1, and alcohol produce combined mitochondrial injury and cytotoxicity in hepatoma cells. *Gastroenterology* 2005; **128**: 96–107.
8. Moriya K, Nakagawa K, Santa T, *et al.* Oxidative stress in the absence of inflammation in a mouse model for hepatitis C virus-associated hepatocarcinogenesis. *Cancer Res* 2001; **61**: 4365–70.
9. Korenaga M, Wang T, Li Y, *et al.* Hepatitis C virus core protein inhibits mitochondrial electron transport and increases reactive oxygen species (ROS) production. *J Biol Chem* 2005; **280**: 37481–8.
10. Lohmann V, Korner F, Koch J, Herian U, Theilmann L, Bartenschlager R. Replication of subgenomic hepatitis C virus RNAs in a hepatoma cell line. *Science* 1999; **285**: 110–3.
11. Ikeda M, Abe K, Dansako H, Nakamura T, Naka K, Kato N. Efficient replication of a full-length hepatitis C virus genome, strain O, in cell culture, and development of a luciferase reporter system. *Biochem Biophys Res Commun* 2005; **329**: 1350–9.
12. Ikeda M, Abe K, Yamada M, Dansako H, Naka K, Kato N. Different anti-HCV profiles of statins and their potential for combination therapy with interferon. *Hepatology* 2006; **44**: 117–25.

13. Setsukinai K, Urano Y, Kakinuma K, Majima HJ, Nagano T. Development of novel fluorescence probes that can reliably detect reactive oxygen species and distinguish specific species. *J Biol Chem* 2003; **278**: 3170–5.
14. Susin SA, Larochette N, Geuskens M, Kroemer G. Purification of mitochondria for apoptosis assays. *Methods Enzymol* 2000; **322**: 205–8.
15. Jarreta D, Orus J, Barrientos A, *et al.* Mitochondrial function in heart muscle from patients with idiopathic dilated cardiomyopathy. *Cardiovasc Res* 2000; **45**: 860–5.
16. Yamamoto A, Hoshi K, Ichihara K. Fluvastatin, an inhibitor of 3-hydroxy-3-methylglutaryl-CoA reductase, scavenges free radicals and inhibits lipid peroxidation in rat liver microsomes. *Eur J Pharmacol* 1998; **361**: 143–9.
17. Jones SP, Teshima Y, Akao M, Marban E. Simvastatin attenuates oxidant-induced mitochondrial dysfunction in cardiac myocytes. *Circ Res* 2003; **93**: 697–9.
18. Cadenas E, Boveris A, Ragan CI, Stoppani AO. Production of superoxide radicals and hydrogen peroxide by NADH-ubiquinone reductase and ubiquinol-cytochrome *c* reductase from beef-heart mitochondria. *Arch Biochem Biophys* 1977; **180**: 248–57.
19. Turrens JF, Boveris A. Generation of superoxide anion by the NADH dehydrogenase of bovine heart mitochondria. *Biochem J* 1980; **191**: 421–7.
20. Turrens JF, Alexandre A, Lehninger AL. Ubisemiquinone is the electron donor for superoxide formation by complex III of heart mitochondria. *Arch Biochem Biophys* 1985; **237**: 408–14.
21. Higuchi M, Proske RJ, Yeh ET. Inhibition of mitochondrial respiratory chain complex I by TNF results in cytochrome *c* release, membrane permeability transition, and apoptosis. *Oncogene* 1998; **17**: 2515–24.
22. Imai Y, Kawata S, Tamura S, *et al.* Relation of interferon therapy and hepatocellular carcinoma in patients with chronic hepatitis C. Osaka Hepatocellular Carcinoma Prevention Study Group. *Ann Intern Med* 1998; **129**: 94–9.
23. Shiratori Y, Imazeki F, Moriyama M, *et al.* Histologic improvement of fibrosis in patients with hepatitis C who have sustained response to interferon therapy. *Ann Intern Med* 2000; **132**: 517–24.
24. Jain SK, Pemberton PW, Smith A, *et al.* Oxidative stress in chronic hepatitis C: not just a feature of late stage disease. *J Hepatol* 2002; **36**: 805–11.
25. Furutani T, Hino K, Okuda M, *et al.* Hepatic iron overload induces hepatocellular carcinoma in transgenic mice expressing the hepatitis C virus polyprotein. *Gastroenterology* 2006; **130**: 2087–98.
26. Hino K, Kitase A, Satoh Y, *et al.* Interferon retreatment reduces or delays the incidence of hepatocellular carcinoma in patients with chronic hepatitis C. *J Viral Hepat* 2002; **9**: 370–6.
27. Hino K, Okita K. Interferon therapy as chemoprevention of hepatocarcinogenesis in patients with chronic hepatitis C. *J Antimicrob Chemother* 2004; **53**: 19–22.
28. Fartoux L, Degos F, Trepo C, *et al.* Effect of prolonged interferon therapy on the outcome of hepatitis C virus-related cirrhosis: a randomized trial. *Clin Gastroenterol Hepatol* 2007; **5**: 502–7.
29. O'Leary JG, Chan JL, McMahon CM, Chung RT. Atorvastatin does not exhibit antiviral activity against HCV at conventional doses: a pilot clinical trial. *Hepatology* 2007; **45**: 895–8.

GASTROENTEROLOGY 2008;134:226–238

BASIC-LIVER, PANCREAS, AND BILIARY TRACT

Hepatitis C Virus–Induced Reactive Oxygen Species Raise Hepatic Iron Level in Mice by Reducing Hepcidin Transcription

SOHJI NISHINA,* KEISUKE HINO,‡ MASAAKI KORENAGA,* CHIARA VECCHI,§ ANTONELLO PIETRANGELO,§ YOICHI MIZUKAMI,‖ TAKAKAZU FURUTANI,* AYA SAKAI,‡ MICHIARI OKUDA,* ISAO HIDAKA,* KIWAMU OKITA,¶ and ISAO SAKAIDA*

*Departments of Gastroenterology and Hepatology and ‡Basic Laboratory Sciences and ‖Center for Gene Research, Yamaguchi University Graduate School of Medicine, Yamaguchi, Japan; ¶Department of Gastroenterology and Hepatology, Shimonoseki Kohsei Hospital, Yamaguchi, Japan; and §Center for Hemochromatosis, Department of Internal Medicine, University of Modena and Reggio Emilia, Modena, Italy

See editorial on page 348.

Background & Aims: **Despite abundant clinical evidence, the mechanisms by which hepatic iron overload develops in patients with hepatitis C virus (HCV)-associated chronic liver disease remain unknown. The aim of this study was to investigate how hepatic iron overload develops in the presence of HCV proteins.** ***Methods:*** **Male transgenic mice expressing the HCV polyprotein and nontransgenic control mice (C57BL/6) were assessed for iron concentrations in the liver, spleen, and serum and iron regulatory molecules in vivo and ex vivo.** ***Results:*** **Transgenic mice had increased hepatic and serum iron concentrations, decreased splenic iron concentration, and lower hepcidin expression in the liver accompanied by higher expression of ferroportin in the duodenum, spleen, and liver. In response to hepatocellular iron excess, transferrin receptor 1 expression decreased and ferritin expression increased in the transgenic liver. Transgenic mice showed no inflammation in the liver but preserved the ability to induce hepcidin in response to proinflammatory cytokines induced by lipopolysaccharide. Hepcidin promoter activity and the DNA binding activity of CCAAT/enhancer-binding protein α (C/EBP) were down-regulated concomitant with increased expression of C/EBP homology protein, an inhibitor of C/EBP DNA binding activity, and with increased levels of reactive oxygen species in transgenic mice at the ages of 8 and 14 months.** ***Conclusions:*** **HCV-induced reactive oxygen species may down-regulate hepcidin transcription through inhibition of C/EBPα DNA binding activity by C/EBP homology protein, which in turn leads to increased duodenal iron transport and macrophage iron release, causing hepatic iron accumulation.**

Hepatic iron overload is one of the pathophysiologic features of hepatitis C virus (HCV)-associated chronic liver disease,[1] even though the level of hepatic iron content is not extremely high.[2] Excess divalent iron can be highly toxic, mainly via the Fenton reaction producing hydroxyl radicals.[3] This is particularly relevant for chronic hepatitis C, in which oxidative stress has been proposed as a major mechanism of liver injury.[4] Oxidative stress and increased iron levels strongly favor DNA damage, genetic instability, and tumorigenesis. Indeed, we have reported that even modest iron supplementation induces hepatocellular carcinoma (HCC) in transgenic mice expressing the HCV polyprotein.[5] Kato et al reported that phlebotomy lowered the risk of progression to HCC,[6] which showed the critical role of iron in the development of HCC in patients with chronic hepatitis C. Thus, there is a critical interaction between HCV proteins and hepatic iron overload in the development of HCV-related HCC. However, the mechanism underlying hepatic iron overload in chronic hepatitis C remains elusive. Chronic inflammation produces proinflammatory cytokines that are involved in iron homeostasis such as tumor necrosis factor (TNF)-α, interleukin (IL)-1β, and IL-6.[7] Because the transgenic mice we have reported[5] do not show any inflammation in the liver, this animal model is suitable for investigating if the expression of HCV protein in the absence of inflammation affects iron metabolism.

Abbreviations used in this paper: C/EBP, CCAAT/enhancer-binding protein; CHOP, C/EBP homology protein; DMT1, divalent metal transporter 1; IL, interleukin; LPS, lipopolysaccharide; ROS, reactive oxygen species; RT-PCR, reverse-transcription polymerase chain reaction; TfR, transferrin receptor; TNF, tumor necrosis factor.

0016-5085/08/$34.00
doi:10.1053/j.gastro.2007.10.011

Table 1. Primers of the Genes Coding Hepcidin, Inflammatory Cytokines, and β-Actin

Gene	Sense	Antisense
Hepcidin	TCCTGCTTCTCCTCCTTGCC[1]	GTCTGCCCTGCTTTCTTCCC[1]
TNF-α	AAGCCTGTAGCCCACGTCGTA[2]	GGCACCACTAGTTGGTTGTCTTTG[2]
IL-1β	TCCAGGATGAGGACATGAGCAC[3]	GAACGTCACACACCAGCAGGTTA[3]
IL-6	CCACTTCACAAGTCGGAGGCTTA[4]	GCAAGTGCATCATCGTTGTTCATAC[4]
β-actin	TGACAGGATGCAGAAGGAGA[5]	GCTGGAAGGTGGACAGTGAG[5]

NOTE. The hepcidin primers are specific for both Hamp1 and Hamp2. GenBank accession numbers are NM_032541 for 1, NM_013693 for 2, NM_008361 for 3, NM_031168 for 4, and NM_007393 for 5.

The aim of this study was to investigate how hepatic iron overload develops in transgenic mice expressing the HCV polyprotein. In the present study, we report that HCV protein-induced reactive oxygen species (ROS) raise hepatic iron level by reducing transcription of hepcidin, a negative regulator of iron release, into the systemic circulation.[8]

Materials and Methods

Animals

The transgene pAlbSVPA-HCV, containing the full-length polyprotein-coding region, under the control of the murine albumin promoter/enhancer was described in detail.[9,10] HCV polyprotein has been shown to be processed into individual proteins in the liver and to be expressed at a biologically relevant level in which transcripts of RNA encoding the complete viral polyprotein are detectable only by reverse-transcription polymerase chain reaction (RT-PCR).[10] Of the 4 transgenic lineages with evidence of RNA transcription of the full-length HCV-N open reading frame (FL-N), the FL-N/35 lineage proved capable of breeding in large numbers. There was no inflammation in transgenic livers.[10] Male FL-N/35 transgenic mice and age-matched C57BL/6 mice were fed a normal rodent diet including carbonyl iron (45-mg/kg diet), bred, maintained, and killed by intraperitoneal injection of 10% pentobarbital sodium preceded by 12-hour fasting according to the criteria outlined in the Guide for the Care and Use of Laboratory Animals.

Histopathologic Procedures

Iron in liver sections was detected by Perls' Prussian blue staining. Ferric iron in the liver sections was histochemically examined using an Iron (II)/Iron (III) Detection kit (Stressgen, Victoria, Canada) with some modification.

Iron Concentrations in Liver, Spleen, and Serum

Iron concentrations in the liver and spleen were measured by atomic absorption spectrometry (Z-6100; Hitachi, Tokyo, Japan), as described previously,[5] and expressed as micrograms Fe per gram of tissue (wet weight). Serum iron concentrations were examined by a colorimetric method and measured with a Quick Auto Neo Fe (Synotest, Tokyo, Japan) according to the manufacturer's instructions.

RNA Isolation and Real-Time RT-PCR

One-step real-time RT-PCR was performed as described previously.[5] The primers amplifying the genes coding hepcidin and inflammatory cytokines are described in Table 1.

Hepatic Levels of Prohepcidin

The protein levels of prohepcidin, an 83-amino acid precursor with strong homology to hepcidin in its C-terminal region,[11] were quantified with a hepcidin prohormone enzyme-linked immunosorbent assay kit (DRG Instruments GmbH, Marburg, Germany) according to the manufacturer's instructions.

Immunohistochemical Detection of Ferroportin

Liver, spleen, and duodenum sections were incubated with a 1:200 dilution of a rabbit polyclonal anti-mouse ferroportin 1 antibody (Alpha Diagnostic International, San Antonio, TX) at 4°C overnight. Following incubation with avidin-conjugated peroxidase (Vecstatin Elite ABC; Vector Laboratories, Burlingame, CA), sections were developed in 3,3′-diaminobenzidine tetrahydrochloride (Sigma Chemical Co, St Louis, MO).

In Situ Detection of ROS

In the presence of ROS, dihydroethidium (Invitrogen Corp, Carlsbad, CA) is oxidized to ethidium bromide and stains nuclei bright red by intercalating with the DNA.[12] Fresh cross sections (10 μm) of unfixed, frozen liver tissues were immediately incubated with 5 μmol/L dihydroethidium at 37°C for 15 minutes in a humidified chamber, subsequently washed twice with ice-cold phosphate-buffered saline, and cover slipped. Fluorescence intensity was quantified using NIH image analysis software for 3 randomly selected areas of digital images in each mouse.

Immunoblotting

Lysates of liver, spleen, and duodenum were separated by sodium dodecyl sulfate/polyacrylamide gel electrophoresis. The proteins were transferred to polyvinylidene difluoride membranes (Millipore, Bedford, MA), blocked overnight at 4°C with 5% skim milk and 0.1% Tween 20 in Tris-buffered saline, and subsequently incubated for 1 hour at room temperature with an anti-mouse ferroportin 1

antibody (Alpha Diagnostic International), anti-mouse divalent metal transporter 1 (DMT1) antibody (Santa Cruz Biotechnology Inc, Santa Cruz, CA), anti-human ferritin antibody (Dako, Glostrup, Denmark), anti-human transferrin receptor (TfR) 1 antibody (Zymed Laboratories, San Francisco, CA), anti-rat CCAAT/enhancer-binding protein α (C/EBPα) antibody (Santa Cruz Biotechnology Inc), or antibacterially expressed, mouse C/EBP homology protein (CHOP) fusion protein antibody (Abcam, Cambridge, England).

Injection of Lipopolysaccharide

Lipopolysaccharide (LPS, 1 μg/g body wt, *Escherichia coli* 0111:B4; Sigma Chemical Co) or an equivalent volume of phosphate-buffered saline was injected intraperitoneally, and liver samples were isolated for RNA preparation 6 hours after injection.

Isolation and Culture of Primary Hepatocytes

Hepatocytes were isolated from FL-N/35 transgenic mice and nontransgenic mice by a 2-step collagenase perfusion procedure. They were then seeded in Williams' medium E (Invitrogen Corp) and supplemented with 10% fetal calf serum, penicillin (100 u/mL)-streptomycin (100 μg/mL) (Invitrogen Corp), and 100 nmol/L insulin. Four hours later, the medium was renewed with the same medium.

Cloning of Mouse Hepcidin Promoter and Construction of Reporter Vectors

The murine hepcidin promoter region was cloned by PCR using mouse DNA as a template and specific hepcidin primers: mHAMPpr_789 fw 5′- GCGCTCGAGGAATACATCGTCAAGCCAGAC-3′ mHAMPpr_318_fw 5′-TTCCTCGAGTCACCAATCCAATCACTGTTTAGG-3′ mHAMPpr_124_fw 5′-GCCCTCGAGGCGCCACTATTTTCTTGGAA-3′ and mHAMPpr_rev 5′-GCGAAGCTTGTGTGGTGGCTGTCTAGGAGC-3′ (the incorporated *Xho*I and *Hin*dIII sites are underlined). PCR products were then purified, digested with *Xho*I/*Hin*dIII, and subcloned in the pGL3-Luc (Promega, Madison, WI) plasmid upstream of the firefly luciferase gene.

Cell Transfection and Luciferase Assay

Primary hepatocytes obtained from 4 mice in each group were transiently transfected with pGL3 Basic vector (negative control), pGL3-CMV vector (positive control), or reporter vectors containing the mouse hepcidin promoter region (pGL3_mHAMP124 [−110/+14], pGL3_mHAMP318 [−304/+14], or pGL3_mHAMP789 [−775/+14]) by using TransFectin Lipid Reagent (Bio-Rad Laboratories Inc, Hercules, CA) 24 hours after cell seeding. The pSV-β-galactosidase control vector encoding β-galactosidase (Promega) used as a cotransfectant served as the control for transfection efficiency. Cellular extracts were analyzed for luciferase activity with a Luciferase assay system (Promega) 48 hours after transfection. β-Galactosidase enzyme assay was performed using the β-galactosidase Enzyme Assay System (Promega). Each assay was performed in duplicate.

Electrophoretic Mobility Shift Assay

Nuclear extracts were obtained using a Nuclear Extraction Kit (Panomics, Redwood, CA), following the manufacturer's instructions. Five micrograms of the nuclear extracts was incubated for 30 minutes at room temperature with horseradish peroxidase–labeled oligonucleotide probe 5′-CATGGATGGTATTGAGAAATCTG-3′ (C/EBP binding site is underlined)[12] using an EMSA Gel-Shift Kit (Panomics) according to the manufacturer's instructions.

Quantification of C/EBP Activation

C/EBPα and C/EBPβ activation was quantified using a Trans AM C/EBP α/β kit (Active Motif, Carlsbad, CA), following the manufacturer's instructions. Briefly, 5 μg of nuclear extract was added to a well to which an oligonucleotide encoding the C/EBP consensus binding site had been immobilized. C/EBPα and C/EBPβ contained in nuclear extract were detected by an antibody directed against either C/EBPα or C/EBPβ.

Statistical Analysis

Quantitative values are expressed as mean ± SD. Two groups at each time point were compared by the Student *t* test. Two groups among multiple groups were compared by the rank-based, Kruskal–Wallis analysis of variance test followed by Scheffe's test. A *P* value of less than .05 was considered significant.

Results

Increased Iron Levels in Liver and Serum and Decreased Iron Level in Spleen

FL-N/35 transgenic mice fed a normal rodent diet had greater hepatic iron contents at the ages of 8 ($P < .05$) and 14 months ($P < .05$) than nontransgenic mice (Figure 1*A*). Serum iron levels were also significantly greater in FL-N/35 transgenic mice at the ages of 8 ($P < .05$) and 14 months ($P < .01$) (Figure 1*B*). Transferrin saturation was significantly greater in FL-N/35 transgenic mice than in nontransgenic mice at the ages of 8 (55.1% ± 12.1% vs 40.2% ± 12.0%; $P < .05$) and 14 months (47.3 ± 8.6 vs 35.8 ± 5.6; $P < .05$). In contrast, splenic iron content was significantly lower in FL-N/35 transgenic mice at the ages of 8 ($P < .05$) and 14 months ($P < .01$) (Figure 1*C*). Thus, it appeared that hepatic iron accumulation in FL-N/35 transgenic mice likely resulted from increased intestinal iron absorption and/or increased iron release from macrophages.

As shown in Figure 1*D*, FL-N/35 transgenic mice had histologically mild but clear iron accumulation in the liver as compared with nontransgenic mice (Figure 1*D*, I and II). Immunohistochemical analysis and high

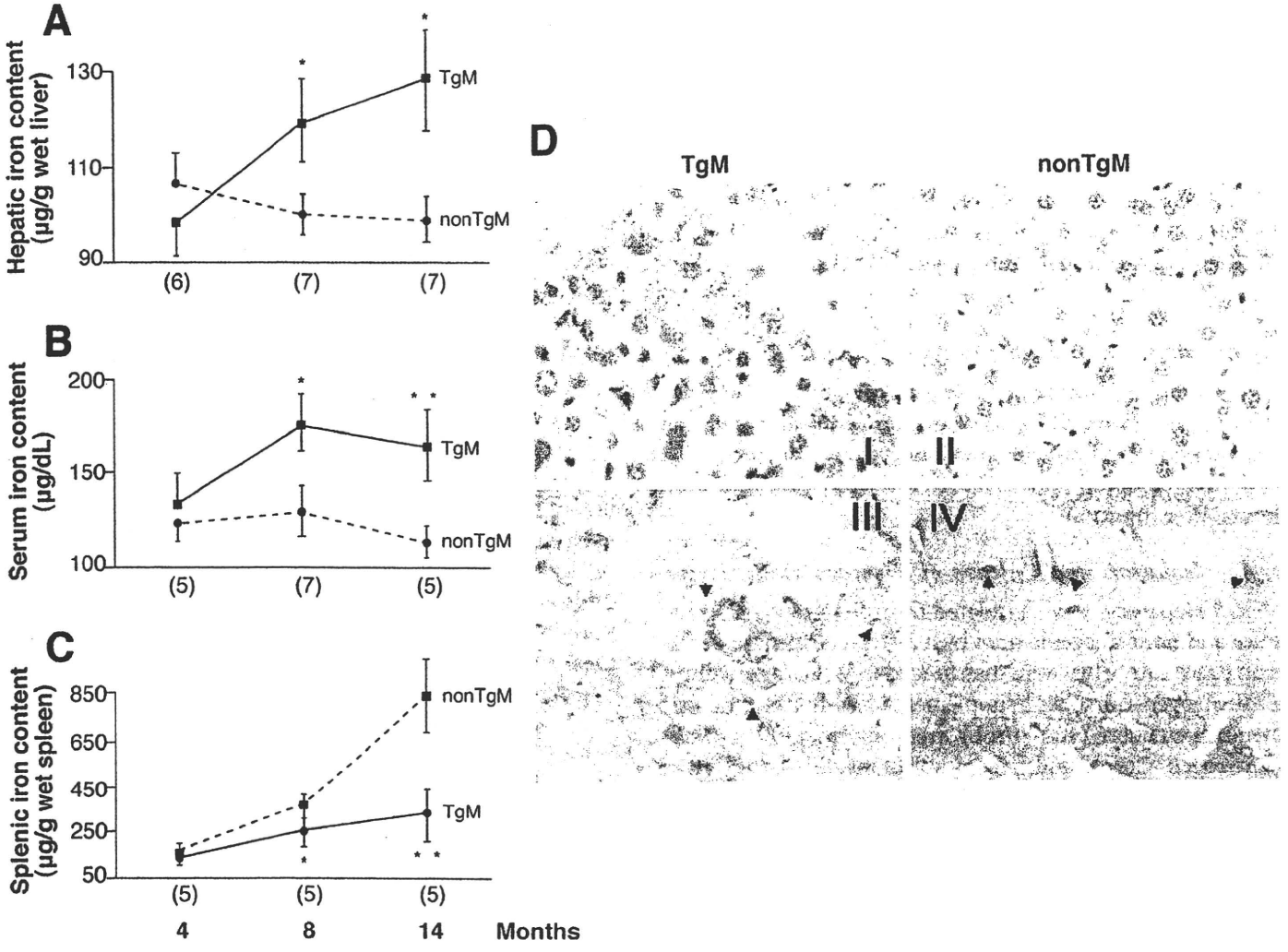

Figure 1. Iron concentrations in the liver, serum, and spleen and iron localization in the liver. (*A*) Hepatic and (*C*) splenic iron concentrations were measured by atomic absorption spectrometry in mice at the ages of 4, 8, and 14 months. (*B*) Serum iron levels were measured using a colorimetric method. $^{*}P < .05$, $^{**}P < .01$ versus same-age nontransgenic mice (nonTgM). The numbers in parentheses represent the number of animals examined in each group. (*D*) Iron in liver sections was examined by Perls' Prussian blue staining (I and II: original magnification 400×) and by immunohistochemical method in TgM and nonTgM (III and IV: original magnification 1000×) at the age of 8 months. *Arrows* indicate the sinusoidal lining cells. TgM, FL-N/35 transgenic mice.

magnification made it possible to differentiate iron localization in sinusoidal lining cells from that in hepatocytes. Ferric iron was localized in both hepatocytes and sinusoidal lining cells but was predominantly present in hepatocytes in FL-N/35 transgenic mice (Figure 1*D*, III and IV).

Hepcidin Levels in Liver

Because there is no known regulatory mechanism for iron excretion, systemic iron homeostasis is maintained by tight regulation of intestinal iron absorption and macrophage iron release.[13] Although the mechanism for this remains to be fully elucidated, hepcidin, a peptide hormone secreted by the liver,[8] seems to have a key role. Hepatic hepcidin messenger RNA (mRNA) levels were significantly lower in FL-N/35 transgenic mice at the ages of 8 ($P < .05$) and 14 months ($P < .01$) (Figure 2*A*). Similarly, protein levels of prohepcidin were significantly lower in FL-N/35 transgenic mice at the ages of 8 ($P < .05$) and 14 months ($P < .01$) (Figure 2*B*). These results suggested that hepatic iron accumulation was closely associated with decreased hepcidin expression in the transgenic mice.

Expression of Ferroportin in Duodenum, Spleen, and Liver

Hepcidin binds to the iron exporter ferroportin, which results in internalization and degradation of ferroportin.[14] Diminished hepcidin expression, therefore, is expected to lead to stabilization of ferroportin, with increased mobilization of iron from macrophages and, presumably, increased intestinal uptake as well. As shown in Figure 3*A*, several clusters of cells stained positively for ferroportin were present in the duodenum, spleen, and liver in FL-N/35 transgenic mice, whereas such clusters were nearly absent in all 5 nontransgenic mice at the age

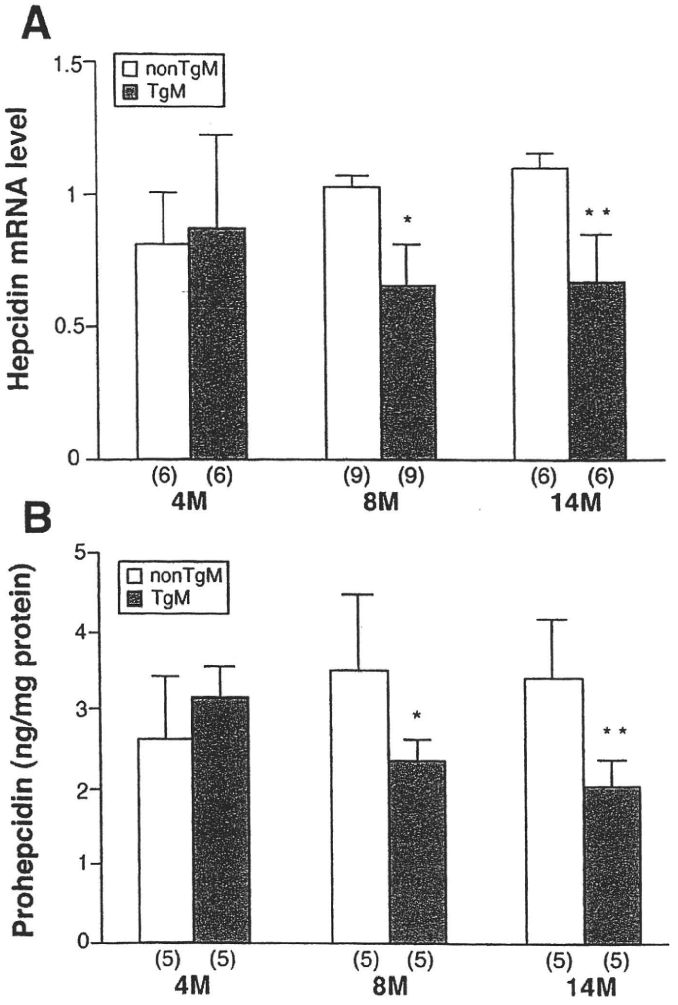

Figure 2. Hepatic levels of hepcidin mRNA and prohepcidin. The expression levels of (*A*) hepcidin mRNA and (*B*) prohepcidin were measured by real-time RT-PCR and enzyme-linked immunosorbent assay, respectively. The relative quantities of hepcidin mRNA in the liver were normalized to β-actin mRNA. The relative protein levels of prohepcidin were normalized by protein concentrations and expressed as nanogram per milligram protein. $^{*}P < .05$ (8 months) and $^{**}P < .01$ (14 months) versus same-age nontransgenic mice (nonTgM). The numbers in parentheses represent the number of animals examined in each group. TgM, FL-N/35 transgenic mice.

of 14 months. Hepatic expression of ferroportin was found in both hepatocytes and sinusoidal lining cells, probably Kupffer cells, with predominant localization in sinusoidal lining cells (Figure 3*A*). The expression of ferroportin in the duodenum, spleen, and liver was greater in FL-N/35 transgenic mice at the age of 8 and/or 14 months (Figure 3*B*). Hepatic expression of ferroportin did not appear to increase to the same degree as expression in the duodenum and spleen (Figure 3*B*).

Expression of DMT1 in Duodenum and Liver

DMT1 is an apical iron transporter in the duodenum and may participate in the uptake of non-transferrin-bound iron by hepatocytes.[15] The expression of DMT1 in the duodenum and liver was similar in FL-N/35 transgenic mice and nontransgenic mice (Figure 4) at the ages of 4, 8, and 14 months. Because transferrin saturation was approximately 50% at the ages of 8 and 14 months in FL-N/35 transgenic mice, it is unlikely that non-transferrin-bound iron contributed significantly to circulating iron. Our results suggested that an increase in DMT1 protein in either duodenum or liver was not required for hepatic iron accumulation in FL-N/35 transgenic mice.

Expression of Ferritin and TfR1 in Liver

Intracellular iron excess inhibits the binding of iron regulatory proteins to iron-responsive elements in the 5′-untranslated region of ferritin mRNA and 3′-untranslated region of TfR1 mRNA, which allows the translation of ferritin mRNA and decreases the stability of TfR1 mRNA.[16] Ferritin consists of H subunits and L subunits that assemble to form a shell of 24 subunits with a cavity capable of storing up to 4500 Fe atoms as hydrous ferric oxide polymers.[17] As shown in Figure 5*A*, the expression of L subunits of ferritin was significantly greater in FL-N/35 transgenic mice than in nontransgenic mice at the ages of 8 ($P < .01$) and 14 months ($P < .05$). Although H subunits could not be detected, this was consistent with the results of experimentally iron-overloaded C57BL/6 mice.[18] H subunits of ferritin in the liver may be difficult to detect with the anti-ferritin antibody used in both studies.

We next measured the expression of TfR1 in the liver to assess if it showed appropriate iron-dependent regulation. As shown in Figure 5*B*, the expression of TfR1 protein was significantly lower in FL-N/35 transgenic mice at the ages of 8 and 14 months ($P < .01$).

Hepcidin Expression in Response to Inflammation

Hepcidin expression is enhanced by iron overload and inflammation.[7,11] We next examined if the present animal model preserved the ability to induce hepcidin in response to inflammation. Induction of acute inflammation by LPS injection led to significant up-regulation of TNF-α, IL-1β, and IL-6 in the liver in both FL-N/35 transgenic mice and nontransgenic mice. With up-regulation of inflammatory cytokines, hepatic hepcidin expression was significantly increased by LPS injection in both FL-N/35 transgenic mice and nontransgenic mice (Figure 5*C*).

Promoter Activity of Hepcidin

To study the effects of HCV proteins on the transcriptional regulation of hepcidin, reporter gene assays were performed for primary mouse hepatocytes. Two reporter vectors, pGL3_mHAMP318 and pGL3_mHAMP789, exhibited significantly lower luciferase activity in FL-N/35 transgenic hepatocytes than in nontransgenic hepatocytes at the ages of 8 and 14 months ($P < .05$) (Figure 6*B*). Thus, the transcriptional activity of hepcidin was

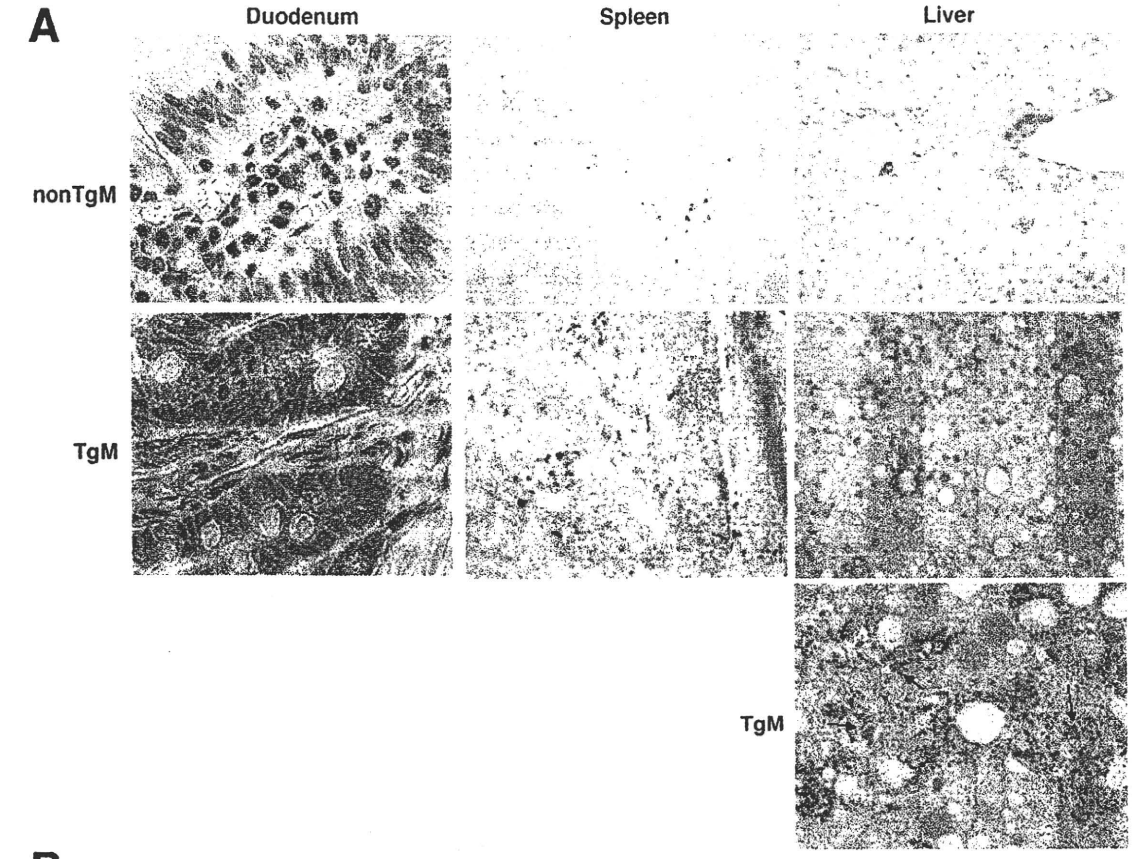

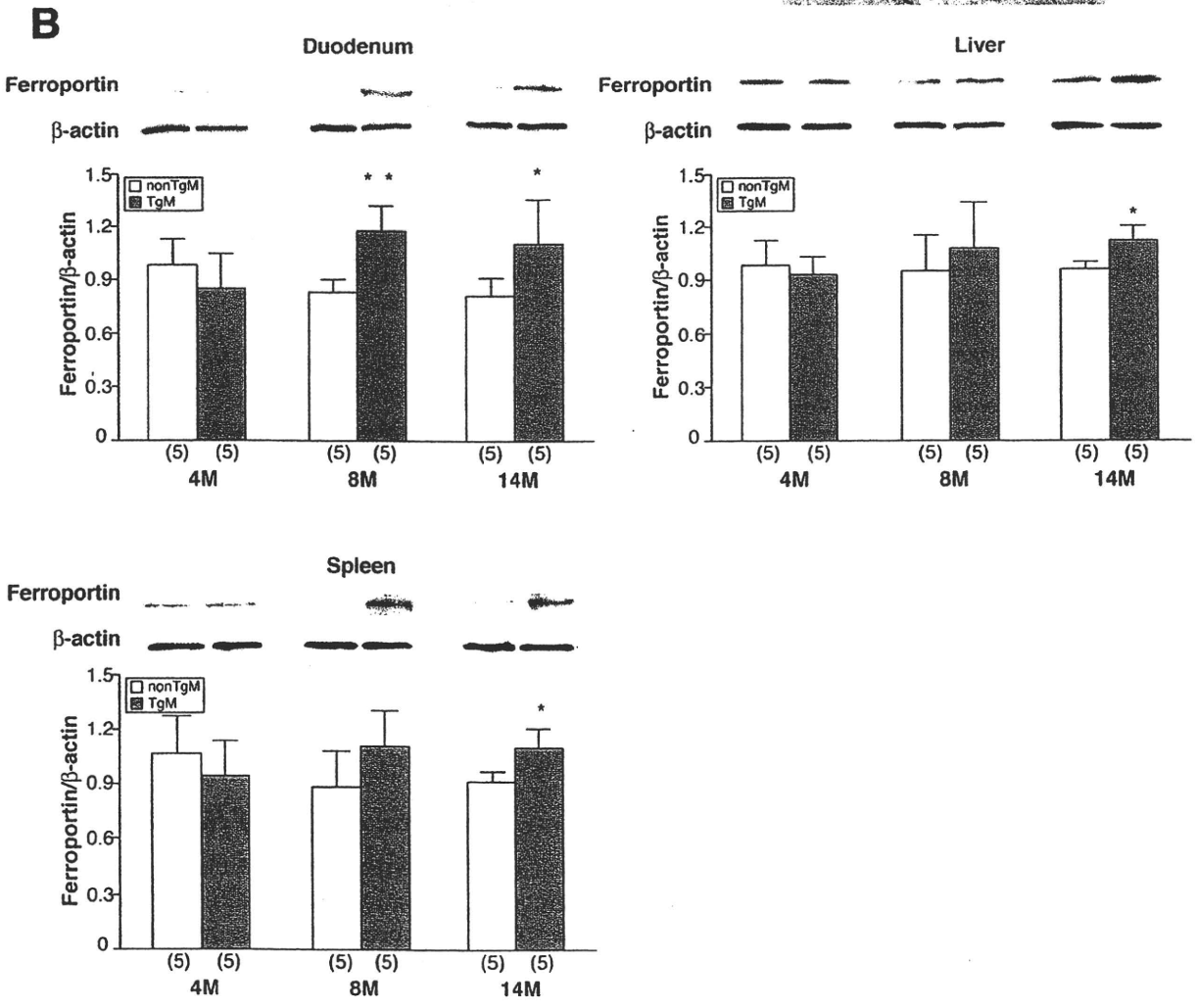

Figure 3. Expression of ferroportin in duodenum, spleen, and liver. (*A*) Immunohistochemical detection of ferroportin in duodenum, spleen, and liver in mice at the age of 14 months (original magnification 1000× for duodenum, 400× for spleen, 400× and 1000× for liver). *Arrows* indicate the sinusoidal lining cells. (*B*) Immunoblots for ferroportin were performed using duodenum, spleen, and liver lysates. The degree of protein expression was normalized with β-actin. The *numbers in parentheses* represent the number of animals examined in each group. $^{*}P < .05$, $^{**}P < .01$ versus same-age nontransgenic mice (nonTgM). TgM, FL-N/35 transgenic mice.

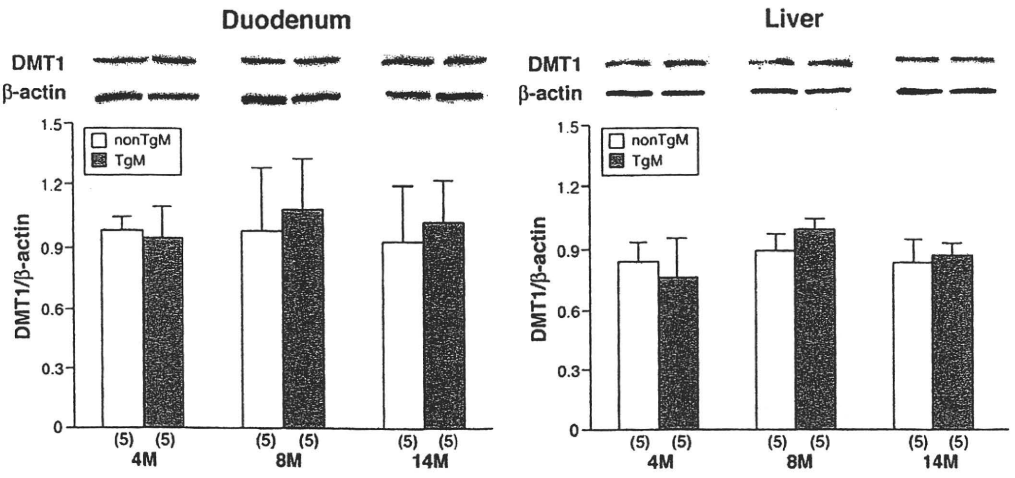

Figure 4. Expression of DMT1 in duodenum and liver. Immunoblots for DMT1 were performed using duodenum and liver lysates obtained from mice in each group. The degree of protein expression was normalized with β-actin. The *numbers in parentheses* represent the number of animals examined in each group. TgM, FL-N/35 transgenic mice.

reduced in FL-N/35 transgenic hepatocytes. The reporter vectors pGL3_mHAMP124, pGL3_mHAMP318, and pGL3_mHAMP789 harbor 1, 2, and 3 putative binding sites for the transcription factor C/EBP, respectively (Figure 6*A*). These results suggested that the middle putative C/EBP binding site was critical for hepcidin promoter activity and were consistent with a previous report that deletion of DNA containing the middle putative C/EBP binding site strongly decreased hepcidin promoter activity.[19]

DNA Binding Activity of C/EBPα

We next examined if the reduced transcriptional activity of hepcidin resulted from decreased DNA binding activity of C/EBP. As expected, DNA binding activity of C/EBP was clearly suppressed in FL-N/35 transgenic mice as compared with that in nontransgenic mice at the age of 8 months (Figure 7*A*). This DNA binding was specific because it was efficiently suppressed by addition of a 100-fold molar excess of the unlabeled wild-type C/EBP oligonucleotide probe as a competitor. We further quantified activation of C/EBPα and C/EBPβ using mouse nuclear extracts. DNA binding activity of C/EBPα was significantly reduced in FL-N/35 transgenic mice compared with nontransgenic mice at the age of 8 months ($P < .05$), but not at the age of 4 months, whereas the binding activity of C/EBPβ was similar in transgenic and nontransgenic mice at the ages of 4 and 8 months (Figure 7*B*). C/EBPα protein levels did not differ in transgenic and nontransgenic mice at the ages of 8 and 14 months (Figure 7*C*). Thus, reduction of C/EBPα DNA binding rather than its expression appeared to be the underlying cause of the down-regulated hepcidin promoter activity in FL-N/35 transgenic mice.

Expression of CHOP

CHOP is a nuclear protein that inhibits C/EBP activity by preventing its DNA binding to the promoter of a subset of genes.[20] We next examined the expression of CHOP to investigate if this protein was associated with reduction of DNA binding activity of C/EBPα in FL-N/35 transgenic mice. The hepatic expression of CHOP was significantly increased in FL-N/35 transgenic mice compared with nontransgenic mice at the ages of 8 and 14 months (Figure 7*D*). CHOP may have decreased DNA binding activity of C/EBPα in the FL-N/35 transgenic mice.

ROS Generation

There have been several lines of evidence that ROS up-regulate the expression of CHOP.[21] We therefore evaluated in situ ROS production by staining with dihydroethidium to assess if the increased CHOP expression was related to the abundance of ROS production. ROS production was significantly higher in FL-N/35 transgenic mice than in nontransgenic mice at the ages of 8 and 14 months (Figure 7*E*) and paralleled the expression of CHOP. The increased ROS production in the presence of HCV proteins was consistent with a previous report[4] by us.

Discussion

FL-N/35 transgenic mice showed not only hepatic iron accumulation but also an increase in serum iron and a decrease in splenic iron content. They were consistent with reported increases in serum iron and ferritin levels in a large cohort of patients with chronic hepatitis C.[22] The decrease in the hepatic prohepcidin level in FL-N/35 transgenic mice may account for the increase in serum iron and decrease in splenic iron content. Prohepcidin has been shown to be involved in the regulation of iron

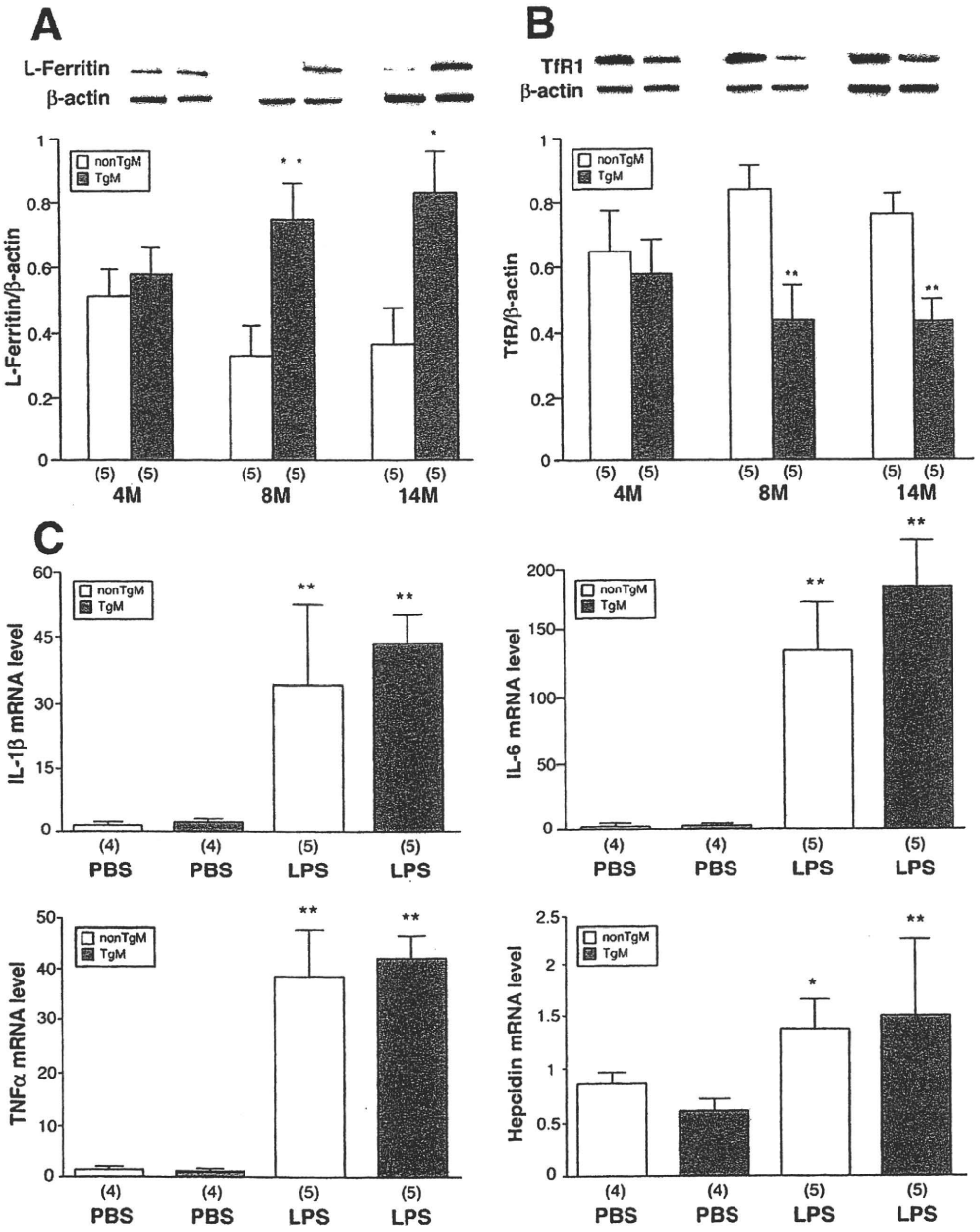

Figure 5. Expression of ferritin, TfR1, and LPS-induced inflammatory cytokines and hepcidin. Immunoblots for (*A*) ferritin and (*B*) TfR1 were performed on liver lysates. The degree of protein expression was normalized with β-actin. *$P < .05$ versus same-age nontransgenic mice (nonTgM), **$P < .01$ versus same-age nonTgM. (*C*) The effect of LPS on the mRNA levels of TNF-α, IL-1β, and IL-6 as well as hepcidin were measured by real-time RT-PCR in mice at the age of 8 months. The relative quantities of target mRNA in the liver were normalized with β-actin mRNA. *$P < .05$ versus nonTgM injected with phosphate-buffered saline, **$P < .01$ versus nonTgM injected with phosphate-buffered saline or TgM injected with phosphate-buffered saline. The *numbers in parentheses* represent the number of animals examined in each group. TgM, FL-N/35 transgenic mice.

metabolism in hereditary hemochromatosis, chronic renal insufficiency, and renal anemia,[23] even though there is some controversy regarding the validity of this measurement.[24]

There also remains uncertainty as to whether iron predominantly accumulates in hepatocytes or the reticuloendothelial system, mainly Kupffer cells, in patients with chronic hepatitis C. Some clinical studies found that iron was mainly localized in the reticuloendothelial system,[1,25] whereas others reported its localization in hepatocytes.[26] Interestingly, Fiel et al documented that even ribavirin-associated hemolysis deposited iron preferentially in hepatocytes in patients with chronic hepatitis C.[27] Although ferric iron localized in both hepatocytes and sinusoidal lining cells in FL-N/35 transgenic and nontransgenic mice, hepatocytic localization was more predominant in FL-N/35 transgenic mice (Figure 1*D*). This is consistent with the observed decrease in hepcidin expression in FL-N/35 mice. Patients and mice with hemochromatosis mutations causing low hepcidin expression have iron accumulation predominantly in hepatocytes.[28] Low hepcidin expression in these situations is

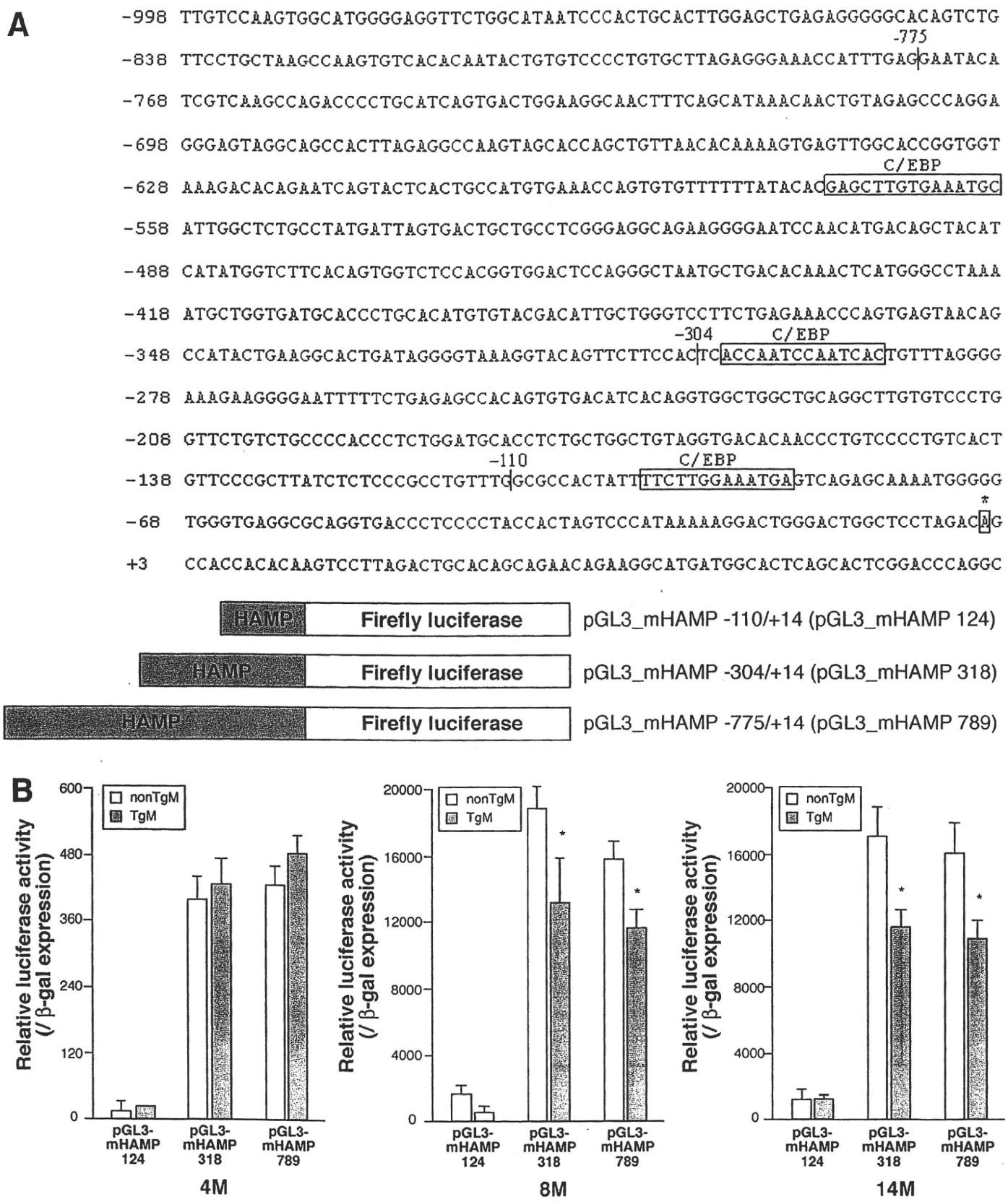

Figure 6. Nucleotide sequence of mouse hepcidin promoter region, schematics of reporter vectors, and luciferase activity of primary hepatocytes transfected with mouse hepcidin promoter constructs. (*A*) The putative start of transcription is indicated by an *asterisk* and is designated +1. Sequences surrounded by *boxes* indicate potential binding sites for transcription factor C/EBP. The reporter vectors pGL3_mHAMP124, pGL3_mHAMP318, and pGL3_mHAMP789 contain 124, 318, and 789 base pairs of the mouse hepcidin promoter region, respectively. (*B*) Primary hepatocytes obtained from 4 mice each were transfected with mouse hepcidin promoter constructs. The pSV-β-galactosidase (β-gal) control vector served as the control for transfection efficiency. Luciferase activity was normalized against β-galactosidase activity from the same lysate. Each assay was performed in duplicate. *$P < .05$ versus same-age nontransgenic mice (nonTgM). TgM, FL-N/35 transgenic mice.

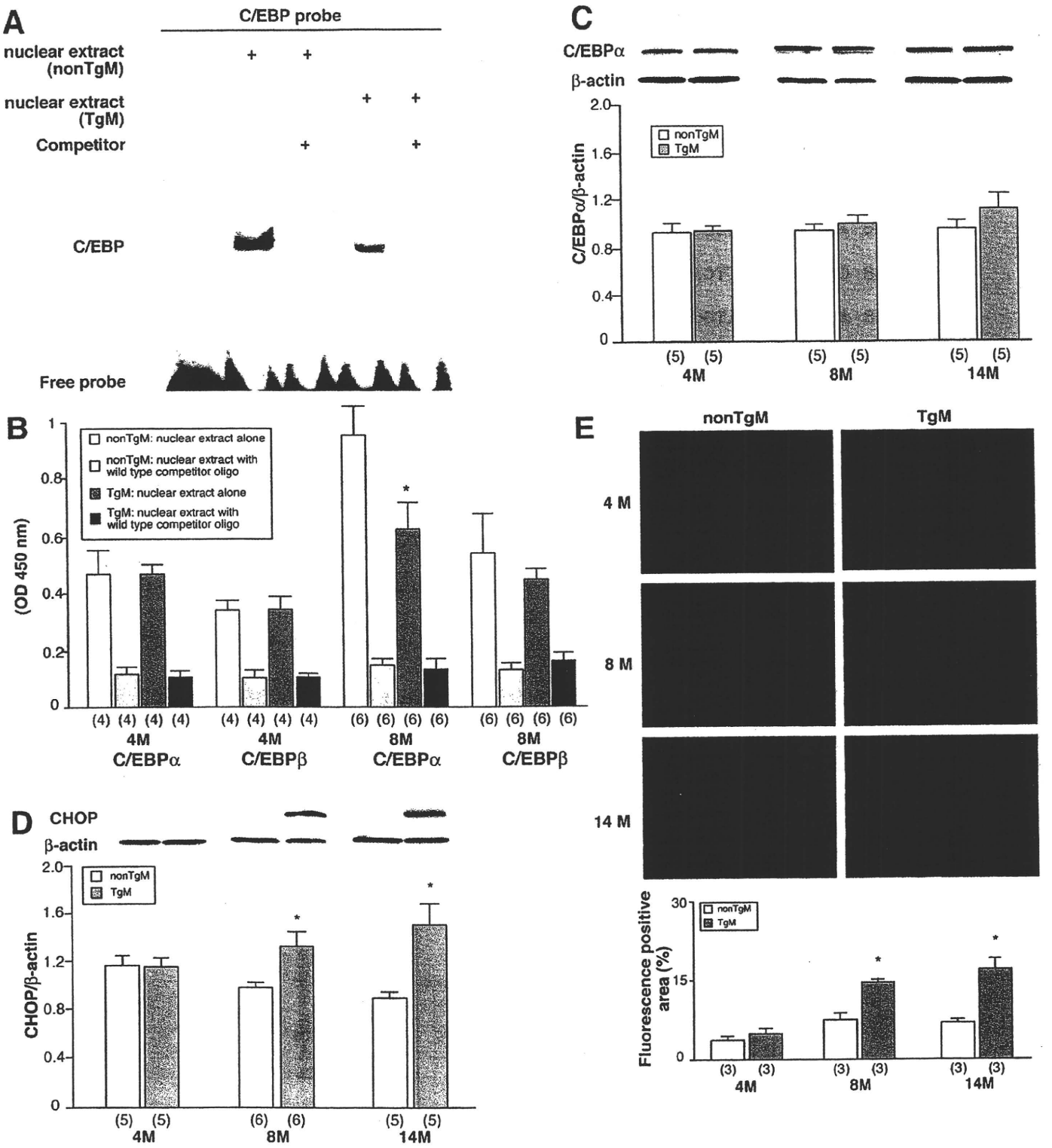

Figure 7. C/EBP binding activity, C/EBPα expression, CHOP expression, and ROS production in liver. (*A*) Electrophoretic mobility shift assay was performed using liver nuclear extracts of mice at the age of 8 months, together with horseradish peroxidase–labeled oligonucleotide probes. Competition experiments were performed by addition of a 100-fold molar excess of the unlabeled wild-type C/EBP oligonucleotide probe. (*B*) DNA binding activity of C/EBPα and C/EBPβ was quantified using liver nuclear extracts of mice, together with the immobilized oligonucleotide on the plate and antibodies to C/EBPα and C/EBPβ. Competition experiments were performed by addition of the wild-type consensus oligonucleotide. *$P < .05$ versus same-age nontransgenic mice (nonTgM) without addition of the wild-type consensus oligonucleotide. Immunoblots for (*C*) C/EBPα and (*D*) CHOP were performed using liver lysates. The degree of protein expression was normalized with β-actin. *$P < .05$ versus same-age nonTgM. (*E*) Frozen liver sections of mice in each group were stained with dihydroethidium. Fluorescence intensity was quantified by NIH image analysis software for 3 randomly selected areas of digital images for each mouse. *$P < .001$ versus same-age nonTgM. The numbers in parentheses represent the number of animals examined in each group. TgM, FL-N/35 transgenic mice.

also associated with increased ferroportin protein levels in duodenum and spleen, with a resultant increase in intestinal iron absorption and a lower splenic iron content.[28] The implications of the increase in hepatic ferroportin expression in FL-N/35 mice are uncertain. The iron-export function of ferroportin may depend on the cell type; it is likely substantial in cells like splenic macrophages that are involved in massive iron turnover and may be marginal in other cell types (such as hepatocytes) that contribute to a much lesser extent to the daily iron traffic into the bloodstream. In the present study, the hepatic expression of ferroportin in FL-N/35 mice did not appear to increase to the same degree as expression in the duodenum and spleen.

Intracellular iron excess inhibits the binding of iron regulatory proteins to iron-responsive elements in the 5′-untranslated region of ferritin mRNA and 3′-untranslated region of TfR1 mRNA, which allows the translation of ferritin mRNA and decreases the stability of TfR1 mRNA.[16] An increase in hepatic ferritin protein and a decrease in TfR1 protein were found in FL-N/35 transgenic mice. Thus, these proteins involved in iron uptake and storage were coordinately regulated, preserving the iron regulatory protein/iron-responsive element regulatory system and not primary causes for hepatic iron overload in these mice. Instead, uptake of transferrin-bound iron through a nonTfR1 pathway[29] may have contributed to excess iron uptake of hepatocytes in the transgenic mice.

Luciferase assay revealed that the hepcidin promoter activity was significantly reduced in FL-N/35 transgenic mice. The IL-6-gp130/signal transducer and activator of transcription (STAT) signal transduction has been shown to be involved in regulating hepcidin transcription.[30] However, this pathway was unlikely to be associated with down-regulation of hepcidin in the present study, because inflammatory cytokines induced by LPS significantly increased hepcidin expression in FL-N/35 transgenic mice. Another signal transduction pathway to hepcidin is the TGF-β/bone morphogenetic protein superfamily[31] and this regulation is strongly potentiated by hemojuvelin, the protein mutated in the most common form of juvenile hemochromatosis.[32] In the future, it will be of interest to evaluate whether HCV polyprotein affects bone morphogenetic protein signaling to hepcidin. The transcription factor C/EBPα has been shown to be involved in regulating hepcidin transcription.[19] Electrophoretic mobility shift assay clearly indicated the reduced DNA binding activity of C/EBP in FL-N/35 transgenic mice. The significant decrease in DNA binding activity of C/EBPα, but not C/EBPβ, was further confirmed by quantifying activation of C/EBPα and C/EBPβ. The C/EBP family contains a conserved carboxy terminal domain consisting of a basic region and an adjacent helical structure. CHOP has strong sequence similarity to C/EBP proteins within the carboxy terminal domain and contains 2 prolines substituting for 2 residues in the basic region, critical for binding to DNA.[20] Thus, heterodimers of CHOP and C/EBP protein are unable to bind their cognate DNA enhancer elements. Therefore, the increased expression of CHOP may account for the reduction of DNA binding activity of C/EBPα in FL-N/35 transgenic mice. Several reports indicated that ROS up-regulate the transcription of CHOP.[21] In the present study, we found significantly higher production of ROS in FL-N/35 transgenic mice than in nontransgenic mice. ROS may explain the increased expression of CHOP in FL-N/35 transgenic mice. ROS production also increased as the mice got older, irrespective of the presence of HCV proteins. This result suggests the importance of aging for inducing oxidative stress in the absence of inflammation or evident fibrosis within the liver. As to C/EBPα activity, this result was consistent with a previous observation that ROS induced by alcohol inhibited C/EBPα activity but not C/EBPβ activity.[12] The reason for the lack of C/EBPβ involvement in the repression of hepcidin transcriptional activity in response to alcohol-induced[12] or HCV-induced ROS production (this report) is unclear and needs further investigation. Thus, the mechanisms by which hepatic iron accumulates in the presence of HCV proteins appear to have some similarities with alcohol-induced iron overload. Given that increases in serum iron and occasional iron accumulation in the liver are common to several liver diseases, it is important to assess whether the alteration in iron metabolism seen in the transgenic mice is a specific effect of HCV. Lipid-induced changes in intracellular iron homeostasis in C57BL/6 mice[33] have been shown. We did not find any differences in hepatic triglyceride contents between transgenic and nontransgenic mice. Oxidative stress induced by HCV may be critical for causing iron accumulation in HCV infection.

The present animal model is characterized by a lack of hepatic inflammation, which is different from what is observed in patients with chronic hepatitis C. Serum levels of IL-6 have been shown to be elevated in patients with HCV-related chronic liver disease,[34] which raises the possibility that IL-6 acts to stimulate hepcidin expression through the STAT3 pathway.[30] This would be expected to counteract the decrease in hepcidin expression caused by HCV-induced ROS. However, chronic inflammation with production of proinflammatory cytokines has the potential to deliver an additional burden of ROS, which would be expected to reinforce the decrease in hepcidin expression. In addition, most data on IL-6/LPS activation of hepcidin expression are based on in vitro studies or "acute" inflammation models in vivo. These studies made it possible to categorize hepcidin as a classic "acute phase" response protein. Most likely, during chronic inflammatory states in vivo, the regulation of hepcidin expression is more complex and may depend on many variables, including the particular stage of systemic and/or hepatic inflammatory disease. This might explain the variations in hepatic iron concentrations reported among patients with HCV-related chronic liver disease. Thanks to the absence of inflammation, our transgenic

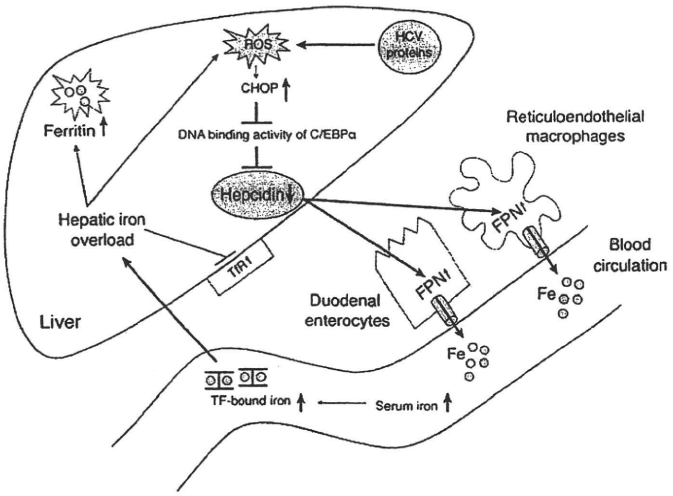

Figure 8. Schematic diagram depicting the mechanisms underlying the hepatic iron accumulation in transgenic mice expressing the HCV polyprotein. HCV protein-induced ROS increase hepatic expression of CHOP and subsequently reduce DNA binding activity of C/EBPα, which leads to reduction of hepcidin transcription. Decreased hepcidin expression enhances ferroportin (FPN) expression in the duodenum and macrophages, resulting in increased duodenal iron transport and macrophage iron release, which lead to hepatic iron accumulation.

animal model allowed us to directly test the role of HCV proteins in iron accumulation without confounding factors.

In conclusion, the current observations support a schema, outlined in Figure 8, whereby HCV protein-induced ROS increase hepatic expression of CHOP and subsequently reduce DNA binding activity of C/EBPα, which causes hepatic iron accumulation through inhibition of hepcidin transcription. These findings may have implications for the hepatic iron accumulation observed in patients with HCV-related chronic liver disease in association with an increased risk of hepatocarcinogenesis.

References

1. Farinati F, Cardin R, De Maria N, et al. Iron storage, lipid peroxidation and glutathione turnover in chronic anti-HCV positive hepatitis. J Hepatol 1995;22:449–456.
2. Di Bisceglie AM, Axiotis CA, Hoofnagle JH, et al. Measurements of iron status in patients with chronic hepatitis. Gastroenterology 1992;102:2108–2113.
3. Fenton HJH. Oxidation of tartaric acid in presence of iron. J Chem Soc 1894;65:899–910.
4. Okuda M, Li K, Beard MR, et al. Mitochondrial injury, oxidative stress, and antioxidant gene expression are induced by hepatitis C virus core protein. Gastroenterology 2002;122:366–375.
5. Furutani T, Hino K, Okuda M, et al. Hepatic iron overload induces hepatocellular carcinoma in transgenic mice expressing the hepatitis C virus polyprotein. Gastroenterology 2006; 130:2087–2098.
6. Kato J, Kobune M, Nakamura T, et al. Normalization of elevated hepatic 8-hydroxy-2'-deoxyguanosine levels in chronic hepatitis C patients by phlebotomy and low iron diet. Cancer Res 2001; 61:8697–8702.
7. Nemeth E, Rivera S, Gabayan V, et al. IL-6 mediates hypoferremia of inflammation by inducing the synthesis of the iron regulatory hormone hepcidin. J Clin Invest 2004;113:1271–1276.
8. Park CH, Valore EV, Waring AJ, et al. Hepcidin, a urinary antimicrobial peptide synthesized in the liver. J Biol Chem 2001;276; 7806–7810.
9. Beard MR, Abell G, Honda M, et al. An infectious molecular clone of a Japanese genotype 1b hepatitis C virus. Hepatology 1999; 30:316–324.
10. Lerat H, Honda M, Beard MR, et al. Steatosis and liver cancer in transgenic mice expressing the structural and nonstructural proteins of hepatitis C virus. Gastroenterology 2002;122:352–365.
11. Pigeon C, Ilyin G, Courselaud B, et al. A new mouse liver-specific gene, encoding a protein homologous to human antimicrobial peptide hepcidin, is overexpressed during iron overload. J Biol Chem 2001;276:7811–7819.
12. Harrison-Findik DD, Schafer D, Klein E, et al. Alcohol metabolism-mediated oxidative stress down-regulates hepcidin transcription and leads to increased duodenal iron transporter expression. J Biol Chem 2006;281:22974–22982.
13. Hentze MW, Muckenthaler MU, Andrews NC. Balancing acts: molecular control of mammalian iron metabolism. Cell 2004; 117:285–297.
14. Nemeth E, Tuttle MS, Powelson J, et al. Hepcidin regulates cellular iron efflux by binding to ferroportin and inducing its internalization. Science 2004;306:2090–2093.
15. Chua AC, Olynyk JK, Leedman PJ, et al. Nontransferrin-bound iron uptake by hepatocytes is increased in the Hfe knockout mouse model of hereditary hemochromatosis. Blood 2004;104:1519–1525.
16. Hentze MW, Kuhn LC. Molecular control of vertebrate iron metabolism: mRNA-based regulatory circuits operated by iron, nitric oxide, and oxidative stress. Proc Natl Acad Sci U S A 1996;93: 8175–8182.
17. Boyd D, Vecoli C, Belcher DM, et al. Structural and functional relationships of human ferritin H and L chains deduced from cDNA clones. J Biol Chem 1985;260:11755–11761.
18. Theurl I, Ludwiczek S, Eller P, et al. Pathways for the regulation of body iron homeostasis in response to experimental iron overload. J Hepatol 2005;43:711–719.
19. Courselaud B, Pigeon C, Inoue Y, et al. C/EBPalpha regulates hepatic transcription of hepcidin, an antimicrobial peptide and regulator of iron metabolism. Cross-talk between C/EBP pathway and iron metabolism. J Biol Chem 2002;277:41163–41170.
20. Ron D, Habener JF. CHOP, a novel developmentally regulated nuclear protein that dimerizes with transcription factors C/EBP and LAP and functions as a dominant-negative inhibitor of gene transcription. Genes Dev 1992;6:439–453.
21. Bek MF, Bayer M, Muller B, et al. Expression and function of C/EBP homology protein (GADD153) in podocytes. Am J Pathol 2006;168:20–32.
22. Shan Y, Lambrecht RW, Bonkovsky HL. Association of hepatitis C virus infection with serum iron status: analysis of data from the third National Health and Nutrition Examination Survey. Clin Infect Dis 2005;40:834–841.
23. Kulaksiz H, Gehrke SG, Janetzko A, et al. Pro-hepcidin: expression and cell specific localisation in the liver and its regulation in hereditary haemochromatosis, chronic renal insufficiency, and renal anaemia. Gut 2004;53:735–743.
24. Kemna E, Pickkers P, Nemeth E, et al. Time-course analysis of hepcidin, serum iron, and plasma cytokine levels in humans injected with LPS. Blood 2005;106:1864–1866.
25. Bonkovsky HL, Banner BF, Rothman AL. Iron and chronic viral hepatitis. Hepatology 1997;25:759–768.
26. Brunt EM. Pathology of hepatic iron overload. Semin Liver Dis 2005;25:392–401.
27. Fiel MI, Schiano TD, Guido M, et al. Increased hepatic iron deposition resulting from treatment of chronic hepatitis C with ribavirin. Am J Clin Pathol 2000;113:35–39.

28. Pietrangelo A. Hereditary hemochromatosis—a new look at an old disease. N Engl J Med 2004;350:2383–2397.
29. Thorstensen K, Trinder D, Zak O, et al. Uptake of iron from N-terminal half-transferrin by isolated rat hepatocytes. Evidence of transferrin-receptor-independent iron uptake. Eur J Biochem 1995;232:129–133.
30. Pietrangelo A, Dierssen U, Valli L, et al. STAT3 is required for IL-6-gp130-dependent activation of hepcidin in vivo. Gastroenterology 2007;132:294–300.
31. Wang RH, Li C, Xu X, et al. A role of SMAD4 in iron metabolism through the positive regulation of hepcidin expression. Cell Metab 2005;2:399–409.
32. Babitt JL, Huang FW, Wrighting DM, et al. Bone morphogenetic protein signaling by hemojuvelin regulates hepcidin expression. Nat Genet 2006;38:531–539.
33. Van Lenten BJ, Prieve J, Navab M, et al. Lipid-induced changes in intracellular iron homeostasis in vitro and in vivo. J Clin Invest 1995;95:2104–2110.
34. Migita K, Abiru S, Maeda Y, et al. Serum levels of interleukin-6 and its soluble receptors in patients with hepatitis C virus infection. Hum Immunol 2006;67:27–32.

Received May 3, 2007. Accepted September 27, 2007.

Address requests for reprints to: Keisuke Hino, MD, PhD, Department of Basic Laboratory Sciences, Yamaguchi University Graduate School of Medicine, 1-1-1 Minami-Kogushi, Ube, Yamaguchi 755-8505, Japan. e-mail: k.hino@yamaguchi-u.ac.jp; fax: (81) 836-222824.

The authors report that no conflicts of interest exist.

Supported by grants from the Ministry of Education, Culture, Sports, Science and Technology (15590653 and 18590736) and in part by the Ministry of Health, Labor and Welfare, Japan, and by a grant from EEC Framework 6 (LSHM-CT-2006-037296 EuroIron1).

The authors thank Dr Stanley M. Lemon for kindly providing the transgenic mice and Dr Tokuhiro Ishihara for assistance with histologic preparation.

平成4年7月20日第3種郵便物認可　毎月1回30日発行
19巻2号（通巻211号）平成21年1月30日発行　ISSN 1344-6940

鉄代謝と鉄過剰症

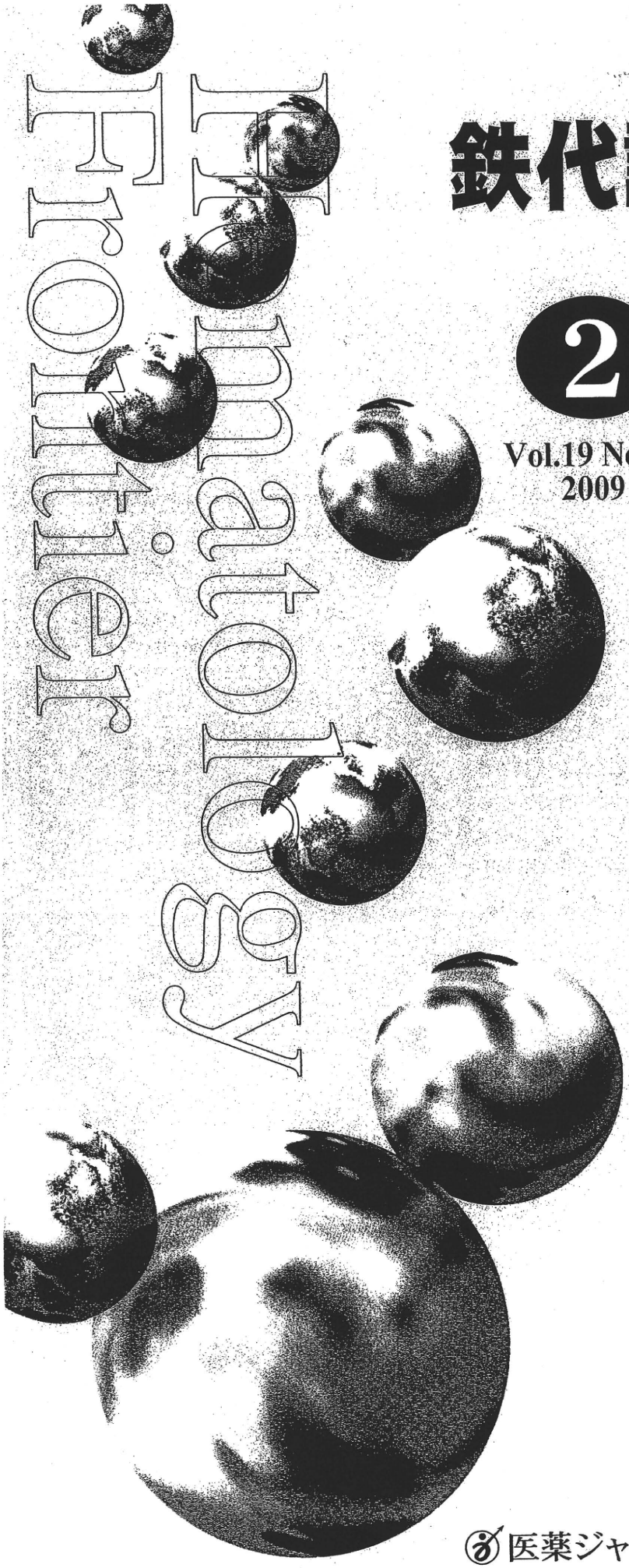

2
Vol.19 No. 2
2009

血液フロンティア
Hematology Frontier

特集

連載

医薬ジャーナル社